Accident Analysis and Prevention 171 (2022) 106670

Contents lists available at ScienceDirect

Accident Analysis and Prevention

journal homepage: www.elsevier.com/locate/aap

Beyond gaze fixation: Modeling peripheral vision in relation to speed, Tesla Autopilot, cognitive load, and age in highway driving

Shiyan Yang [a,*], Kyle Wilson [a,b], Trey Roady [a], Jonny Kuo [a], Michael G. Lenné [a]

[a] Seeing Machines, 80 Mildura St, Fyshwick 2609 ACT, Australia
[b] Department of Psychology, University of Huddersfield, West Yorkshire, UK

ARTICLE INFO

Keywords:
Peripheral vision
Useful field
Tesla Autopilot
Cognitive load
Highway driving
Bayesian regression model

ABSTRACT

Objective: The study aims to model driver perception across the visual field in dynamic, real-world highway driving.
Background: Peripheral vision acquires information across the visual field and guides a driver's information search. Studies in naturalistic settings are lacking however, with most research having been conducted in controlled simulation environments with limited eccentricities and driving dynamics.
Methods: We analyzed data from 24 participants who drove a Tesla Model S with Autopilot on the highway. While driving, participants completed the peripheral detection task (PDT) using LEDs and the N-back task to generate cognitive load. The I-DT (identification by dispersion threshold) algorithm sampled naturalistic gaze fixations during PDTs to cover a broader and continuous spectrum of eccentricity. A generalized Bayesian regression model predicted LED detection probability during the PDT—as a surrogate for peripheral vision—in relation to eccentricity, vehicle speed, driving mode, cognitive load, and age.
Results: The model predicted that LED detection probability was high and stable through near-peripheral vision but it declined rapidly beyond 20°-30° eccentricity, showing a narrower useful field over a broader visual field (maximum 70°) during highway driving. Reduced speed (while following another vehicle), cognitive load, and older age were the main factors that degraded the mid-peripheral vision (20°-50°), while using Autopilot had little effect.
Conclusions: Drivers can reliably detect objects through near-peripheral vision, but their peripheral detection degrades gradually due to further eccentricity, foveal demand during low-speed vehicle following, cognitive load, and age.
Applications: The findings encourage the development of further multivariate computational models to estimate peripheral vision and assess driver situation awareness for crash prevention.

1. Introduction

The road safety elements of peripheral vision have been studied for several decades. Peripheral vision is associated with rods (photoreceptor cells sensitive to low light levels) in the human retina and covers 99.9% of the visual field (i.e., the space in which objects are visible during a gaze fixation; Aulhorn & Harms, 1972; Traquair, 1927). Since it has poor acuity and color perception, drivers who process on-road information through peripheral vision have worse lane keeping performance (e.g., Summala et al., 1996) and delayed braking reaction to the lead vehicle (e.g., Lamble et al., 1999; Wolfe et al., 2019). However, a recent theory proposed by Wolfe et al. (2020) states a positive role of peripheral vision in driving that was rarely considered: it supports driver information acquisition from the scene and guides search for specific information. This theory is rooted in the Texture Tiling Model, according to which peripheral input over sizable regions of the visual field is efficiently encoded as a set of summary statistics (e.g., marginal distribution of luminance, luminance autocorrelation) in the brain. According to this model, peripheral vision retains imperfect but sufficient information to enable rapid scene perception and understanding (Rosenholtz et al., 2012a; b).

The missing role of peripheral vision in the development of driver monitoring systems (DMS) has recently been discussed by researchers. For example, Wolfe et al. (2020) noted that current DMS estimates

* Corresponding author at: 80 Mildura St, Fyshwick 2609 ACT, Australia.
E-mail address: shiyan.yang@seeingmachines.com (S. Yang).

https://doi.org/10.1016/j.aap.2022.106670
Received 14 November 2021; Received in revised form 6 April 2022; Accepted 8 April 2022
Available online 13 April 2022

driver attention allocation, in-part, by assessing where the driver is looking in relation to pre-determined regions known as "areas of interest". The determination of where the driver is looking is largely based on drivers' foveal vision, which links to a small central pit of human retina (fovea) with the highest density of cones (photoreceptor cells responsible for color vision, as opposed to rods). Thus, DMS, in its current state, does not estimate peripheral vision, and could be oversensitive to any eccentric gaze behavior and thereby oversimplify this behavior as distraction (European Commission, 2021).

How we should capture peripheral vision computationally using DMS remains an open question. The Texture Tiling model represents a state-of-art approach to quantify the representations of peripheral regions as a set of summary statistics, which mimics how humans recognize peripheral patterns (Rosenholtz et al., 2012b). However, computations in this model are time consuming, so the model is yet to be practical for driver monitoring research. This paper, therefore, focuses on more measurable aspects of peripheral vision—detection of targets with different eccentricities across the visual field. Higher detection probability may illustrate the *useful field* (or referred to as the functional visual field; Wolfe, 2021), which is defined as the total visual field area in which useful information can be acquired within one eye fixation (Ball et al., 1988). It may also inspire the improvements of driver distraction detection algorithms, such as implementing eccentricity-contingent distraction thresholds.

Driver peripheral vision is usually measured with a dual-task paradigm that consists of a task that demands foveal vision and another task that requires detecting peripheral objects. One typical setting is to detect fixed artificial stimuli at eccentric locations, such as letters or numbers in the Useful Field of View (UFOV) test (Atchley & Dressel, 2004; Ball et al., 1988; Williams, 1985), LEDs (light emitting diodes) in the peripheral detection task (PDT; Jahn et al., 2005; van Winsum, 2018), or gaze-contingent eccentric stimuli (Gaspar et al., 2016). Another setting requires participants to fixate on an eccentric visual task, using peripheral vision to detect driving-relevant events on a computer screen, such as the lead car's deceleration (Lamble et al., 1999) or brake lights (Wolfe et al., 2019). Detection probability or reaction time corresponding to discrete peripheral angles is measured and used to infer peripheral perception. Abundant studies have shown that cognitive load degrades peripheral vision, resulting in either *tunnel vision* (i.e., large decrements in visual performance with increasing retinal eccentricity; Ringer et al., 2016; Williams, 1985), or *general interference* (i.e., general degradation of extrafoveal perception regardless of its eccentricity to foveal vision; Crundall et al., 2002; Savage et al., 2019; van Winsum, 2018; Williams, 1982; 1988). Age is also a well-studied factor degrading peripheral vision (Ball et al., 1988; Owsley, 2011; Savage et al., 2019).

However, these measures of peripheral vision were predominantly conducted in simulation environments, in which participants only receive artificial visual cues (e.g., color, contrast) in computer graphics (Svärd et al., 2021), and may not experience realistic vehicle dynamics (e.g., longitudinal control). Thus, it remains unknown how vehicle dynamics affect peripheral vision. When the vehicle slows down due to car following on highways, peripheral vision may be worse as the result of higher attentional demands for headway assessment and longitudinal control, so peripheral vision should be estimated in relation to vehicle dynamics in the real world.

Few studies have considered the role of peripheral vision in automated driving, which tempts drivers to be "out-of-the-loop" – increasingly having their eyes off the road and hands off the wheel (Merat et al., 2019). When gaze deviates from the road, peripheral vision may still enable the search for ambient visual cues that communicate important information, such as takeover requests or upcoming vehicle actions, to support takeover performance and situation awareness (e.g., Borojeni et al., 2016; Karjanto et al., 2018). Quantifying peripheral perception over the visual field can help designers to optimize the specifications (e.g., location) of ambient displays, so that drivers, even with more off-road glances, are likely to be kept in the loop.

Previous laboratory approaches of assessing peripheral vision, such as displaying gaze-contingent stimuli or manipulating gaze fixations, are neither practical nor safe for replication in on-road environments. Advances in DMS offer a better option. DMS can precisely track gaze direction and if an object can be located in the same coordinate system as gaze direction, its eccentricity can be calculated relative to the moving gaze. This can be achieved through synchronized inputs from DMS (tracking gaze) and outward-facing sensors (locating objects), but it is beyond what technologies can offer to date. This research, therefore, adopted some elements in the PDT paradigm – fixed LED stimuli on the vehicle dashboard – to substitute on-road objects so that calculating LEDs' eccentricity became plausible. While drivers operated the vehicle, a fixed LED stimulus was illuminated in their visual field at varying degrees of eccentricity. With sufficient samples of eccentricity (the LED "travels" through the whole visual field), peripheral vision could be modeled based on LED detection corresponding to a spectrum of eccentricity. This overcomes a major limitation of previous studies: few eccentric angles within a small radical extent ($\leq 30^{\circ}$) were explored. Although LED stimuli are not the same as driving-relevant stimuli for peripheral processing (Wolfe et al., 2019), they serve as a baseline for comparison.

This study pursues three aims: to model driver peripheral vision in a broader, continuous visual spectrum; to understand how driving factors, such as speed and assisted driving, affect peripheral vision; and to examine how cognitive load and age affect peripheral vision during real-world driving. Data were collected during highway driving in which participants completed the PDT and auditory N-back tasks (inducing cognitive load) while driving a Tesla Model S with Autopilot. Autopilot is classified as a driver support feature according to the latest SAE (the Society of Automotive Engineers) standards (SAE International, 2021), so driving with Autopilot is called "assisted driving" in this paper. A generalized Bayesian regression model (BRM) was built to predict the detection probability and reaction time of PDT in relation to multiple factors, including eccentricity, speed, driving mode, cognitive load, and age. The model quantified perception over the visual field in dynamic driving environments, providing insight into how peripheral vision can be computationally incorporated into driver monitoring technologies to improve distraction assessment and crash prevention.

2. Method

2.1. Study summary

The study was based on Phase 2 of the automated vehicle research program known as CANdrive. CANdrive was sponsored by the Australian Capital Territory (ACT) Government and sought to better understand how drivers would interact with assistive driving technology in real-world situations. The experimental details were described in Yang et al., 2020.

2.1.1. Participants

Twenty-four ACT residents (12 males, 12 females) with valid full driver licenses participated in the study. Six males (ages: min = 22, mean = 31, max = 38, SD = 5.5) and 7 females (ages: min = 22, mean = 29, max = 35, SD = 5.2) were clustered into the younger group while 6 males (ages: min = 45, mean = 54, max = 68, SD = 8.3) and 5 females (ages: min = 45, mean = 49, max = 51, SD = 2.4) belonged to the older group. Among them, 11 males and 8 females had prior experience operating the same vehicle used here six months beforehand on a test track (see Yang et al., 2021), while the remainder had no prior experience with the Tesla vehicle. Participants were also familiar with adaptive cruise control (ACC) to some extent (based on familiarity ratings they provided from minimum 1 to maximum 7: mean = 3.7, SD = 2.5).

2.1.2. Apparatus

Participants drove a Tesla Model S (2017 version) equipped with

Autopilot 2.0. The vehicle was equipped with a proprietary automotive-grade Driver Monitoring System (DMS, Seeing Machines Ltd, ACT, Australia). This driver facing infrared camera system samples driver head position and facial features (at 46 Hz) to determine driver gaze and attention state. Additionally, two webcams, one Mobileye camera, and one forward-facing camera were installed inside the vehicle for data collection.

2.1.3. Test route and experimental conditions

The test drive was conducted on a local highway during off-peak hours (10–12 AM or 1–3 PM). The repeated highway section was 15 km long with speed limits of either 90 or 100 km/h, did not involve any intersections, and took approximately 10 min to drive one way. Participants had hand(s) on the steering wheel in accordance with the local laws. Before the test drive (for data collection), participants drove a single round trip of the test route. During this time, they were given practice on the secondary tasks and on operating the vehicle's automated features.

The test drive consisted of manual driving (MD) and assisted driving (AD; SAE Level 2) sections. In each section, there were four experimental conditions: 1) baseline (no secondary task); 2) PDT; 3) auditory N-back task; and 4) PDT + N-back task. Two conditions – baseline (no secondary task) and PDT – were combined in one test drive to reduce driving hours and avoid driver fatigue. Thus, there were six test drives in total (~10 min each), conducted in a counterbalanced order according to the Latin square design. The order of the six test drives was balanced among every six participants and repeated four times over twenty-four participants. For modeling peripheral vision, this paper focuses on the experimental conditions with PDT, including MD + PDT, MD + PDT + N-back, AD + PDT, and AD + PDT + N-back.

2.1.4. N-back Task

The N-back task was an auditory delayed letter recall task, as a variant of the original delayed digital recall task (Mehler et al., 2012; Mehler et al., 2011). The task required participants to listen to a string of random English letters presented audibly in a pre-determined random order from a portable speaker on the center console. The number of letters presented in each string varied between 6 and 10, with a 1.5-s interval between consecutive letters. Participants were required to recall the letter two steps back from the present last letter (2-back). They verbally reported the third-last letter from the end of the string. Their report was recorded in a spreadsheet by the experimenter. In each experimental condition, participants completed 10 N-back trials with 10–20 s intervals between trials.

2.1.5. Peripheral-detection task (PDT)

This task required participants to press a button attached to their left index fingertip against the steering wheel (see Fig. 1, left) when they saw a red light from one of the five LEDs on top of the dashboard – a central one above the speedometer, a pair of near-left and near-right ones, and a pair of far-left and far-right ones (see Fig. 1, right). The DMS recorded the start and ending timestamps of each button press and synchronized them with sensing data. LED stimulus duration was 2 s with an interval randomly sampled between 12 and 15 s. Stimulus location was uniformly distributed. LED intensity was empirically adjusted to one of two levels (normal vs. stronger) at the beginning, to ensure and balance visibility in different lighting conditions of cloudy or sunny days. To minimize any safety risks induced by engaging with the PDT while driving, participants were given a formal instruction: Please do not intentionally search for LED activations; you need to respond to the LED stimuli only if you happen to see it.

2.2. Data processing

Sensing data were processed within the 2-s window of each LED stimulus, referred to, here, as an "epoch". Sensing data included gaze direction (for calculating eccentricity), vehicle speed, and vehicle mode (MD or AD). Weather condition was manually annotated from the forward-facing videos. The button press response (whether it was responded to) and reaction time (s) were recorded for each epoch. The

Table 1
Definition, unit, and value of the variables in Bayesian regression model.

Variable		Definition	Unit	Value
Independent	LED Eccentricity	The Euclidean distance between the activated LED and the nearest gaze fixation in the 2D yaw-pitch coordinate (see Fig. 3)	°	0–70
	Vehicle Speed	The mean vehicle speed in each epoch	km/h	≥60
	Driving Mode	Manual driving (MD) or assisted driving (AD), confirmed by the CAN Bus signal in each epoch		MD or AD
	Cognitive load	The cognitive load imposed by an N-back task epoch, confirmed by the correct response from the driver		Yes or No
	Age Group	Younger group between 20 and 40 years and older group above 40 years		Younger or Older
	Weather Condition	Weather condition during the test drive, confirmed using the forward-facing videos		Sunny or Cloudy
Dependent	Button Press	Pressing the response button following LED stimulus activation		Yes or No
	Reaction Time	The interval between the start of a 2-s LED stimulus and the moment of a button press (recorded up to 5 s).	s	0–5

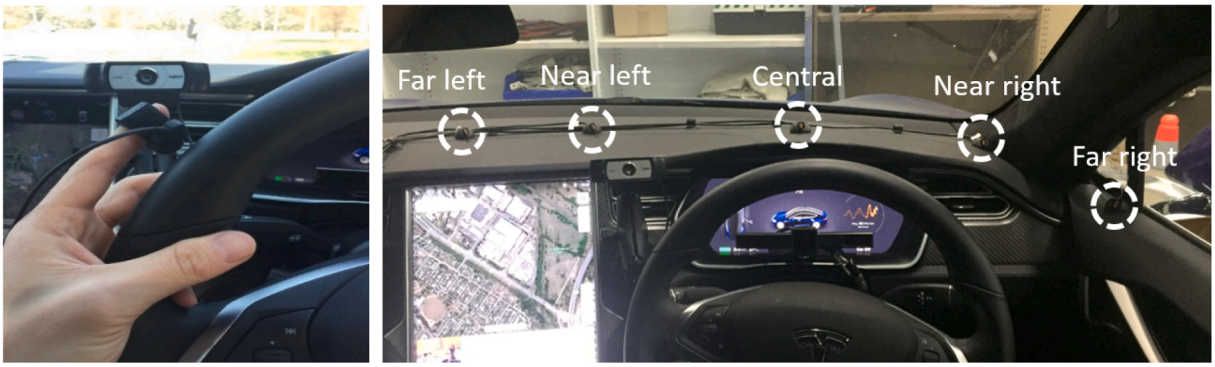

Fig. 1. The touch button on the left index fingertip (left) and the LEDs on the vehicle dashboard (right).

details of these variables are described in Table 1.

Stimulus eccentricity was determined by the LED's location relative to the nearest gaze fixation. Before driving, participants were asked to sit in the stationary vehicle and fixate on each LED. The averaged gaze directions indicated the LEDs' locations in the yaw-pitch coordinate system, whose origin is the location of the DMS camera (see Fig. 2). For the LEDs, the yaw-pitch coordinates (see Fig. 2) were far-left (–33.1°, −8.4°), left (-20.8°, −6.6°), central (1.2°, −7.6°), right (21.6°, −9.9°), and far-right (33.8°, −14.8°).

Gaze fixations were extracted from raw gaze points over each epoch using the I-DT (identification by dispersion threshold) algorithm, which clusters consecutive gaze points with low dispersion (less than the 1.0° threshold) into a fixation (Blignaut, 2009; Salvucci & Goldberg, 2000), with the minimum duration of 100 ms (ISO 15007–1:2014). There could be zero, single, or multiple fixations during an epoch. The pseudocode of the I-DT algorithm is described in Yang et al. (2021). Eccentricity was defined as the Euclidean distance between the activated LED and the nearest gaze fixation during the 2-s epoch (see Fig. 2).

Due to CAN Bus logging issues, two participants' data was excluded from the analysis. Epochs outside the N-back tasks in the MD-PDT + N-back and AD-PDT + N-back conditions were also excluded. Additionally, 16 epochs with vehicle speeds lower than 60 km/h and 2 epochs with zero fixations identified by the I-DT algorithm were excluded. The total 1,374 remaining epochs (391 in MD-PDT, 293 in MD-PDT + N-back, 380 in AD-PDT, and 310 in AD-PDT + N-back) were used for Bayesian regression modeling.

2.3. Bayesian regression modeling

Multi-level Bayesian regression models (BRMs) were built to analyze multiple effects on drivers' detection performance. A BRM estimates the posterior distribution of the population-level effect (parameters β; assumed to be the same across observations) and group-level effect (parameters u; assumed to vary across the grouping variables). Several population-level variables were incorporated into the BRMs, including LED eccentricity ($X_{eccentricity}$), vehicle mode (X_{mode}), cognitive load (X_{CL}), the interaction between cognitive load and eccentricity ($X_{CL}X_{eccentricity}$), age group (X_{age}), vehicle speed (X_{speed}), and weather ($X_{weather}$). The group-level variable was the participant ID (X_{pid}; see Equations (1) and (4)). These variables were linearly combined with corresponding coefficients as the linear predictor η (see Equations (1) and (4)), which links to the mean (μ) of the dependent variable via the link function (logit or log; see Equations (2) and (5)). For the dependent variables, button presses followed a Bernoulli distribution (see Equation (3)) while reaction times followed an exponential distribution (e.g., Whelan, 2008; see Equation (6)).

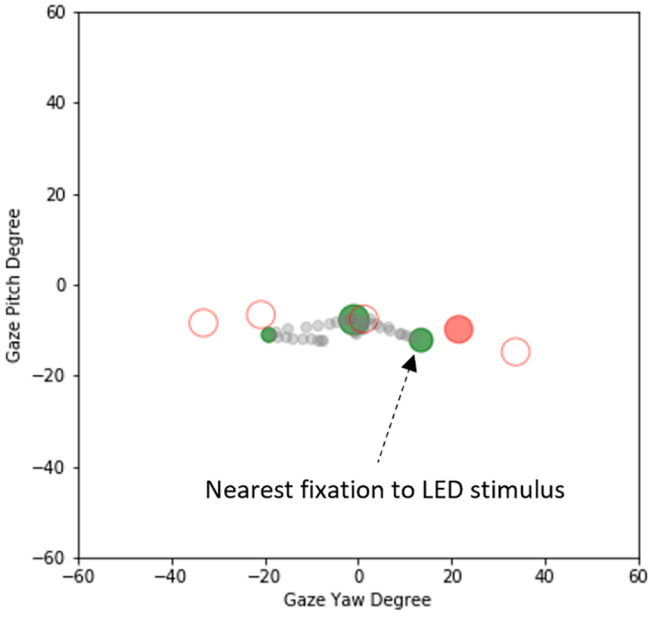

Fig. 2. Gaze fixations (green dots) and saccades (gray dots) during a 2-s epoch. The inactivated LEDs are represented by the red circles while the activated one (near right) is represented by the red dot.

$$\boldsymbol{\eta_{button}} = \beta_{intercept} + \beta_{eccentricity}\boldsymbol{X}_{eccentricity} + \beta_{speed}\boldsymbol{X}_{speed} + \beta_{mode}\boldsymbol{X}_{mode} + \beta_{CL}\boldsymbol{X}_{CL} + \beta_{CL\times E}\boldsymbol{X}_{CL}\boldsymbol{X}_{eccentricity} + \beta_{age}\boldsymbol{X}_{age} + \beta_{weather}\boldsymbol{X}_{weather} + u_{pid}\boldsymbol{Z}_{pid} \quad (1)$$

$$logit(\mu_{button,i}) = \eta_{button,i} \quad (2)$$

$$buttonpress_i \sim Bernoulli(\mu_{button,i}) \quad (3)$$

$$\boldsymbol{\eta_{RT}} = \beta_{intercept} + \beta_{eccentricity}\boldsymbol{X}_{eccentricity} + \beta_{speed}\boldsymbol{X}_{speed} + \beta_{mode}\boldsymbol{X}_{mode} + \beta_{CL}\boldsymbol{X}_{CL} + \beta_{CL\times E}\boldsymbol{X}_{CL}\boldsymbol{X}_{eccentricity} + \beta_{age}\boldsymbol{X}_{age} + \beta_{weather}\boldsymbol{X}_{weather} + u_{pid}\boldsymbol{Z}_{pid} \quad (4)$$

$$log(\mu_{RT,j}) = \eta_{RT,j} \quad (5)$$

$$RT_j \sim Exponential(\mu_{RT,j}) \quad (6)$$

where i = 1, 2, ..., 1374 and j = 1, 2, ..., 904 (epochs with button press).

Posterior distributions of population-level effects (β) were estimated by the NUTS (No-U-Turn Sampler) sampling algorithm (an upgraded version of Hamiltonian Monte Carlo; Hoffman & Gelman, 2014) using the R package "brms" (Bayesian regression models using Stan; Bürkner, 2018). The default improper flat prior was chosen for all β parameters. The NUTS algorithm approximated the posterior distribution of every β using four Markov chains with 2000 samples per chain. The first 1000 samples were used to tune the parameters of this algorithm, and the total 4000 remaining samples were used to estimate the posterior distribution of each β, which was summarized using the mean ("Estimate") and the standard deviation ("Est. Error") with two-sided 89% credible intervals (or percentile intervals; "Lower 89% CI" and "Upper 89% CI"; see Table 2). The accuracy of the fitted BRMs was validated by the efficient approximate leave-one-out cross-validation (LOO) using Pareto smoothed importance sampling (PSIS; Vehtari et al., 2017). The significance of each effect was determined by whether the probability of this effect was more than 89% in one-tailed hypothesis tests. We chose 89% CI instead of 95%, the convention in frequentist statistics, because 95% is less stable for small posterior sample sizes (<10,000; Kruschke, 2014, p. 184) and it encourages readers to conduct unconscious hypothesis tests (McElreath, 2018, p. 58). The analyses were completed in R 4.0.5.

3. Results

3.1. Population-Level effect on detection probability

The prediction accuracy of the fitted BRMs was validated according to Pareto k estimates (using "LOO" function in the "brms" package) and all observations were good (k in (-∞, 0.5]). For LED detection probability (i.e., the expected value of *buttonpress*), the effects of eccentricity (-), speed (+), cognitive load × eccentricity (-), age (+; reference level = older) were significant according to one-tailed hypothesis tests, while for reaction time, only the effect of eccentricity (+) was significant (see Table 2). Here, "+" (or "-") means that this variable positively (or negatively) affected the dependent variable when its value was enlarged (as a continuous variable) or changed from the reference level to the other level (as a categorical variable).

Table 2
Summary of the Population-Level Effects on Detection Probability and Reaction Time.

Effects on Detection probability						
Effect	Parameter	Estimate	Est. Error	Lower 89% CI	Upper 89% CI	One-Tailed Test 89%
Intercept	$\beta_{intercept}$	−1.28	0.97	−2.78	0.28	No
Eccentricity	$\beta_{eccentricity}$	−0.09	0.01	−0.10	−0.07	Sig.
Speed	β_{speed}	0.04	0.01	0.02	0.05	Sig.
Mode	β_{mode}	0.21	0.13	0.00	0.42	Sig.
Cognitive Load	β_{CL}	0.27	0.31	−0.22	0.77	No
CL × Eccentricity	$\beta_{CL\times E}$	−0.03	0.01	−0.06	−0.01	Sig.
Age	β_{age}	0.74	0.42	0.09	1.40	Sig.
Weather	$\beta_{weather}$	0.17	0.42	−0.48	0.84	No
Effects on Reaction Time						
Effect	Parameter	Estimate	Est. Error	Lower 89% CI	Upper 89% CI	One-Tailed Test
Intercept	$\beta_{intercept}$	0.31	0.47	−0.45	1.03	No
Eccentricity	$\beta_{eccentricity}$	0.01	0.00	0.00	0.02	Sig.
Speed	β_{speed}	0.00	0.00	−0.01	0.00	No
Mode	β_{mode}	−0.01	0.07	−0.11	0.10	No
Cognitive Load	β_{CL}	0.05	0.12	−0.14	0.24	No
CL × Eccentricity	$\beta_{CL\times E}$	0.00	0.01	−0.01	0.01	No
Age	β_{age}	−0.09	0.11	−0.26	0.09	No
Weather	$\beta_{weather}$	0.04	0.12	−0.14	0.23	No

Note. "Sig." represents statistically significant.

3.2. Prediction of detection probability

Apart from analyzing the population-level effects, the BRM can also predict the expected value of the dependent variable in relation to a changing independent variable when the remaining independent variables were fixed at either a chosen value or the reference level.

3.2.1. Eccentricity

The detection probability declined with increasing LED eccentricity (see Table 2). For example, the (mean) detection probability dropped gradually from 95.7% to 6.4% as the LED eccentricity increased from 0° to 70° (variables fixed: speed = 90 km/h, driving mode = MD, cognitive load = No, age = younger; see the first plot in the second row in Fig. 3). In this case, 50% detection probability occurred at around 37° of the visual field.

3.2.2. Speed

The detection probability was significantly reduced during lower vehicle speed (than speed limit; see Table 2). Speed strongly affected detection probability at the mid-range of the visual field. The effect was

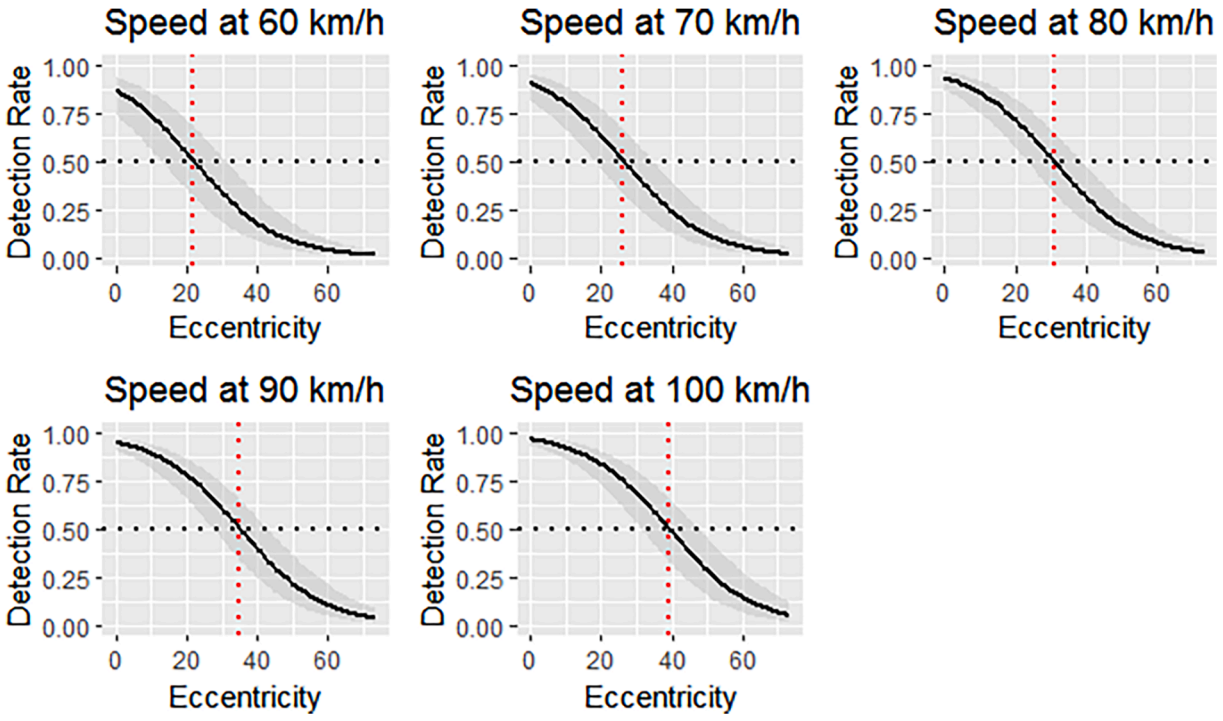

Fig. 3. Detection probability across the visual field at different speed levels (driving mode = MD, cognitive load = No, age = younger). The solid lines represent the mean and the gray regions represent the 89% credible interval. The black horizontal dash line indicates 50% detection rate and the red vertical dash line indicated the eccentricity corresponding to 50% detection rate.

weaker but still apparent at the center and the edge. For example, when speed declined from 100 km/h to 60 km/h, the detection probability declined 26.0% (=64.3%-38.3%) for 30° eccentricity while it only declined 14.6% (=90.6%-76.0%) at 10° and 8.2% (=13.3–5.1%) at 60° eccentricity (variables fixed: driving mode = MD, cognitive load = No, age = younger; see Fig. 3).

3.2.3. Driving mode

The detection probability was significantly higher in manual driving than assisted driving, but only slightly (see Table 2). For instance, in assisted driving the detection probability only dropped by 1.9% (=90.5%−88.6%) at 10°, 4.8% (=64.3%−59.5%) at 30°, and 2.2% (=13.3%−11.1%) at 60° eccentricity (variables fixed: speed = 90 km/h, cognitive load = No, age = younger), the extent to which can barely be perceived (see Fig. 4).

3.2.4. Cognitive load

Cognitive load alone did not significantly affect the detection probability, but its interaction with eccentricity significantly did. Cognitive load did not degrade the detection performance (~90%) when LEDs were near foveal vision, but it worsened the detection of eccentric LEDs beyond ~30° (see red curves in Fig. 4). For example, under cognitive load, the detection probability dropped by 18.6% (from 59.5% to 40.9%) at 30° eccentricity (variables fixed: speed = 90 km/h, driving mode = MD, age = younger; see Fig. 4).

3.2.5. Age

Younger drivers' detection probability was significantly higher than older drivers (see Table 2). The effect of aging was stronger around the mid-range (~20°-50°) than the center and the edge of the visual field. For example, younger drivers' detection was higher than older drivers' by 8.5% (=90.5%- 82.0%) at 10°, 17.6% (=64.3%-46.7%) at 30°, and 6.3% (=13.2%- 6.9%) at 60° eccentricity (variables fixed: speed = 90 km/h, driving mode = MD, cognitive load = No; see Fig. 4).

3.2.6. Weather

Weather did not affect the detection probability (see Table 2) and is not a matter for discussion in this paper.

3.3. Population-Level effect on reaction time

Eccentricity. Reaction time was only sensitive to eccentricity (see Table 2). The larger the eccentricity, the longer the reaction time (see Figure 6). The BRM predicted that the (mean) reaction time increased from 0.86 s to 1.67 s when the eccentricity increased from 0° to 70° (variables fixed: speed = 90 km/h, driving mode = MD, cognitive load = No, age = younger; see Fig. 5).

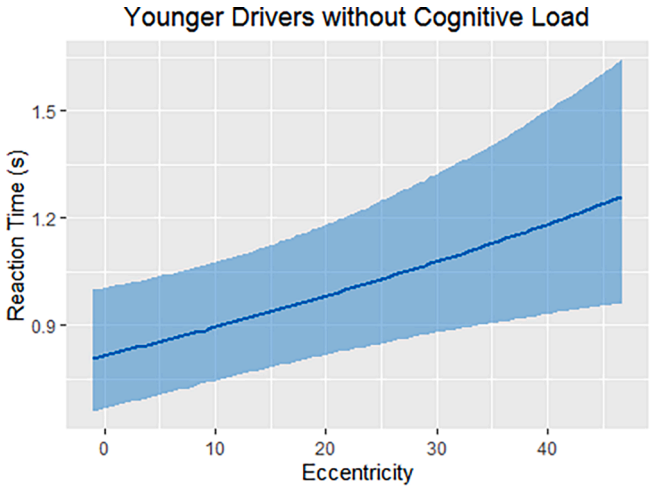

Fig. 5. Reaction time corresponding to eccentricity (speed = 90 km/h, driving mode = MD, cognitive load = No, age = younger). The solid lines represent the mean and the color regions represent the 89% credible interval.

Fig. 4. Detection probability across the visual field (speed = 90 km/h). The solid lines represent the mean and the color regions represent the 89% credible interval.

4. Discussion

Peripheral vision acquires information from the visual field and guides a driver's attention to specific information in the scene, so it is essential for situation awareness in driving (Wolfe et al., 2020). Unlike foveal vision, peripheral vision has not yet been estimated by existing driver monitoring technologies, and few studies have quantified peripheral vision under dynamic conditions in real-world driving. To address this gap, a generalized Bayesian regression model (BRM) was built to model the perception of peripheral vision during the test drive of a Tesla Model S on the highway. The BRM predicted the probability of detecting eccentric LED stimuli—as a surrogate for peripheral perception—in relation to multiple factors, such as eccentricity, vehicle speed, driving mode, cognitive load, and age. The findings provide insight into drivers' perception across the visual field in real-world driving.

The study assessed a broader spectrum of peripheral vision (maximal 70°) than previous studies. When other factors were controlled, the BRM predicted decreased detection probability of LED stimuli (see Fig. 4) and increased reaction time (see Fig. 5) for larger eccentricities. The detection probability was reasonably high within the near periphery, which aligns with recommendations by regulatory bodies globally: information displays should not be located beyond 30° away from the forward roadway (reviewed in Svärd et al., 2021). The detection probability decreased steeply beyond 20°-30° eccentricity, and eventually remained at a low level beyond 50°-60° (see Fig. 4). The slope of descending detection probability may not match with the concept of tunnel vision (steep decline of visual performance with increasing eccentricity), so it is more likely to reflect a narrower useful field. Here, the useful field is not associated with a specific probability threshold to avoid a dichotomous view of the visual field as "useful" and "useless" regions (Wolfe et al., 2017). Drivers may have a narrower useful field in real-world highway driving due to higher foveal demand, compared to the findings from static simulation environments (e.g., Savage et al., 2019; Wolfe et al., 2019). The stable, high detection probability within a certain concentric area of the visual field ($\leq$10°−20°) suggests that a target is still detectable (although not all its details may be perceived) within near periphery, so gaze deviation from the target is not equivalent with complete loss of attention (e.g., drivers may peripherally perceive the forward roadway when they glance at the speedometer). Thus, gaze eccentricity tolerance, to a certain degree, should be considered in the development of gaze-based algorithms for driver distraction or inattention detection, which directly addresses the European Commission's question regarding whether driver distraction warnings should be contingent on gaze eccentricity (European Commission, 2021).

Detection of peripheral LEDs worsened when the vehicle speed declined below the speed limit. As the speed decreased from 90 km/h to 60 km/h, the size of the visual field associated with a greater than 50% detection probability shrank from 37° to 24° (see the red dash lines in Fig. 3). The detection probability decreased unevenly across the visual field, by 9.4% (from 94.5%) at 3° eccentricity, 25.8% (from 64.4%) at 30°, and 8.2% (from 13.4%) at 60° (for younger drivers in manual driving; see Fig. 3). Since 87.4% of the low-speed (<80 km/h) epochs involved close car-following (median headway = 1.2 s), these epochs had higher foveal demand and a narrower useful field. However, Crundall et al. (2002) found general interference (vision degradation regardless of eccentricity) caused by central processing demands from hazard detection, but only within a small range (<7°). The previous and present findings combined suggest that the foveal demands from highway driving may induce a general interference effect on near peripheral vision, and may further degrade mid peripheral vision, narrowing the useful field. When assessing whether a driver is distracted in a case such as this, it may be beneficial to use a threshold with a lower tolerance to object eccentricity.

Drivers had a similar useful field between manual and assisted driving. Although they may often have larger gaze dispersion (Louw & Merat, 2017) and glance more at non-driving related areas (Morando et al., 2021a; b) during vehicle automation, their stable useful field may still enable them to be aware of ambient cues. Ambient in-vehicle displays – which provide light-based cues in drivers' peripheral vision – may offer promise for keeping drivers in the loop during assisted driving (e.g., Borojeni et al., 2016). Our participants, however, only had limited experience with Tesla Autopilot, so further research is needed to measure the useful field of experienced drivers during assisted driving.

According to the BRM, cognitive load does not affect visual perception within 30° of the visual field, but it deteriorates peripheral vision further beyond (see Fig. 4). Many psychology experiments showed general interference, rather than tunnel vision, as a result of cognitive load or distraction (e.g., Crundall et al., 2002; Williams, 1982; 1988). But they only explored a small range (<10°) and did not replicate driving scenarios. The current finding that cognitive load had little influence on near-peripheral vision is supported by other driving studies (e.g., Gaspar et al., 2016). This is more explicitly mentioned in Wolfe et al. (2019): cognitive load has little effect on the detection of the brake light of a lead vehicle at $\leq$30° eccentricity. When the visual field beyond 30° was studied, a novel finding emerged: cognitive load impaired drivers' mid-peripheral vision. This finding, combined with previously found gaze concentration under cognitive load (Reimer, 2009; Victor, Harbluk, & Engström, 2005; Yang et al., 2018), implies the risks of missed or delayed hazard detection from the mid periphery.

Compared to younger drivers, older drivers had similar foveal and near-peripheral vision but worse mid-peripheral perception, which is, again, a sign of smaller useful field. Similarly, Savage et al. (2019) found that older drivers struggled to perceive a more eccentric motorcycle heading to an intersection (in a static image). Since drivers with visual field loss in both eyes had crash rates twice as high compared to those with a normal visual field (Wood, 2002), customizing the prediction of the visual field based on driver age may be appropriate.

LEDs are simple, artificial stimuli, so their detection reflects, at best, some basic aspects of peripheral vision. They may be less generalizable to more complex visual tasks (e.g., object localization and identification), including driving-related tasks. Further research should adapt standard perimetry tasks (e.g., the UFOV test; Wood & Owsley, 2014) in driving contexts to verify the useful field found in this study, and measure how well drivers can perceive driving-relevant objects or cues from the periphery in real-world driving (Wolfe et al., 2019) - the quantification of which could better inform a general-purpose model of peripheral encoding (Rosenholtz, 2016). Moreover, a future model of peripheral perception should separately account for horizontal and vertical eccentricities because they influence the detection probability differently (Lamble et al., 1999). Additionally, peripheral vision should be measured in alternative driving scenarios, for example, in urban driving which features more driving-relevant information (e.g., pedestrians, road signs, and buildings) in drivers' periphery.

5. Conclusion

The paper presents one of the first attempts to assess driver visual field in the real world, responding to the rising awareness of the role of peripheral vision in driver monitoring from academia and industry. A generalized Bayesian regression model was built to predict the detection probability of LEDs with a broader range of eccentricity (maximum 70°). This model showed a narrower useful field – detection probability deteriorating outside the near periphery – as a default state in highway driving, perhaps because of driving-related foveal demand. The mid-range of peripheral vision was reduced the most at low speed (in car-following scenarios), during cognitive load, and in older drivers. Driving automation, however, had little effect on peripheral vision. These quantified relationships, based on real-world data, encourage multivariate computational approaches to estimate driver peripheral vision and better assess situation awareness.

CRediT authorship contribution statement

Shiyan Yang: Conceptualization, Data curation, Formal analysis, Methodology, Software, Validation, Visualization, Writing – original draft, Writing – review & editing. **Kyle Wilson:** Data curation, Methodology, Writing – review & editing. **Trey Roady:** Data curation, Methodology, Writing – review & editing. **Jonny Kuo:** Funding acquisition, Writing – review & editing. **Michael G. Lenné:** Conceptualization, Funding acquisition, Project administration, Writing – review & editing.

Declaration of Competing Interest

The authors declare the following financial interests/personal relationships which may be considered as potential competing interests:

All authors are employees of Seeing Machines, but this publication would not directly associate with their financial situations. The study is part of a project funded by the Australian Capital Territory Government on the purpose of answering scientific questions to benefit the regulation and public perception of automated driving in Australia.

Acknowledgements

We would like to express our special gratitude to Australian Capital Territory (ACT) government for their funding on CANdrive program to benefit the public perception and regulation of automated driving in Australia, and the ACT Automated Vehicle Committee co-chaired by Kate Lundy and Glenn Keys AO for their supervise and guidance on this program. Moreover, we would also like to extend our thanks to Sonal Gupta for support in recruitment, Fivaz Buys for providing hardware support, and Kyle Blay for providing software support.

References

Atchley, P., Dressel, J., 2004. Conversation limits the functional field of view. Hum. Factors 46 (4), 664–673.
Aulhorn, E., Harms, H., 1972. Visual Perimetry. In: Jameson, D., Hurvich, L.M. (Eds.), Visual Psychophysics. Handbook of Sensory Physiology. Springer, Berlin, Heidelberg.
Bürkner, P., 2018. Advanced Bayesian Multilevel Modeling with the R Package brms. R J. 10 (1), 395–411.
Ball, K.K., Beard, B.L., Roenker, D.L., Miller, R.L., Griggs, D.S., 1988. Age and visual search: Expanding the useful field of view. J. Opt. Soc. Am. A, Opt. Image Sci. 5 (12), 2210–2219.
Blignaut, Pieter, 2009. Fixation identification: The optimum threshold for a dispersion algorithm. Attention, Perception, & Psychophysics 71, 881–895.
Borojeni, S.S., Chuang, L., Heuten, W., Boll, S., 2016. Assisting drivers with ambient take-over requests in highly automated driving. In: In *Proceedings of the 8th International Conference on Automotive User Interfaces and Interactive Vehicular Applications*, pp. 237–244.
Crundall, D., Underwood, G., Chapman, P., 2002. Attending to the peripheral world while driving. Appl. Cogn. Psychol. 16 (4), 459–475.
European Commission-Mobility (GROW.I.2). (2021). Report on advanced driver distraction warning systems. Retrieved from https://ec.europa.eu/docsroom/documents/45901?locale=en.
Gaspar, J.G., Ward, N., Neider, M.B., Crowell, J., Carbonari, R., Kaczmarski, H., Ringer, R.V., Johnson, A.P., Kramer, A.F., Loschky, L.C., 2016. Measuring the useful field of view during simulated driving with gaze-contingent displays. Hum. Factors 58 (4), 630–641.
Hoffman, M.D., Gelman, A., 2014. The No-U-Turn sampler: adaptively setting path lengths in Hamiltonian Monte Carlo. J. Mach. Learn. Res. 15 (1), 1593–1623.
Jahn, G., Oehme, A., Krems, J.F., Gelau, C., 2005. Peripheral detection as a workload measure in driving: effects of traffic complexity and route guidance system use in a driving study. Transp. Res. Part F: Traffic Psychol. Behav. 8 (3), 255–275.
Kruschke, J. (2014). Doing Bayesian data analysis: A tutorial with R, JAGS, and Stan (pp.184).
Karjanto, J., Yusof, N.M., Wang, C., Terken, J., Delbressine, F., Rauterberg, M., 2018. The effect of peripheral visual feedforward system in enhancing situation awareness and mitigating motion sickness in fully automated driving. Transp. Res. Part F: Traffic Psychol. Behav. 58, 678–692.
Lamble, D., Kauranen, T., Laakso, M., Summala, H., 1999. Cognitive load and detection thresholds in car following situations: safety implications for using mobile (cellular) telephones while driving. Accid. Anal. Prev. 31 (6), 617–623.
Louw, T., Merat, N., 2017. Are you in the loop? Using gaze dispersion to understand driver visual attention during vehicle automation. Transp. Res. Part C: Emerg. Technol. 76, 35–50.
McElreath, R. (2018). *Statistical rethinking: A Bayesian course with examples in r and stan*. Chapman (pp. 58). Hall/CRC.
Mehler, B., Reimer, B., Coughlin, J.F., 2012. Sensitivity of physiological measures for detecting systematic variations in cognitive demand from a working memory task: an on-road study across three age groups. Hum. Factors 54 (3), 396–412.
Mehler, B., Reimer, B., Dusek, J.A., 2011. MIT AgeLab delayed digit recall task (n-back). Massachusetts Institute of Technology, Cambridge, MA, p. 17.
Morando, A., Gershon, P., Mehler, B., Reimer, B., 2021a. A model for naturalistic glance behavior around Tesla Autopilot disengagements. Accid. Anal. Prev. 161, 106348.
Morando, A., Gershon, P., Mehler, B., & Reimer, B. (2021b). Visual attention and steering wheel control: From engagement to disengagement of Tesla Autopilot. In *Proceedings of the Human Factors and Ergonomics Society Annual Meeting, 65*(1), 1390-1394.
Merat, N., Seppelt, B., Louw, T., Engström, J., Lee, J.D., Johansson, E., Green, C.A., Katazaki, S., Monk, C., Itoh, M., McGehee, D., Sunda, T., Unoura, K., Victor, T., Schieben, A., Keinath, A., 2019. The "out-of-the-loop" concept in automated driving: proposed definition, measures and implications. Cogn. Technol. Work 21 (1), 87–98.
Owsley, C., 2011. Aging and vision. Vision Res. 51 (13), 1610–1622.
Reimer, B., 2009. Impact of cognitive task complexity on drivers' visual tunneling. Transp. Res. Rec. 2138 (1), 13–19.
Rosenholtz, R., 2016. Capabilities and limitations of peripheral vision. Annu. Rev. Vision Sci. 2 (1), 437–457.
Rosenholtz, R., Huang, J., Ehinger, K.A., 2012a. Rethinking the role of top-down attention in vision: Effects attributable to a lossy representation in peripheral vision. Front. Psychol. 3, 13.
Rosenholtz, R., Huang, J., Raj, A., Balas, B.J., Ilie, L., 2012b. A summary statistic representation in peripheral vision explains visual search. J. Vis. 12 (4), 14.
Ringer, R.V., Throneburg, Z., Johnson, A.P., Kramer, A.F., Loschky, L.C., 2016. Impairing the useful field of view in natural scenes: tunnel vision versus general interference. J. Vis. 16 (2), 7.
SAE International. (2021). *SAE levels of driving automation refined for clarity and international audience* (Technical report No. J3016). Retrieved from https://www.sae.org/blog/sae-j3016-update.
Svärd, M., Bärgman, J., Victor, T., 2021. Detection and response to critical lead vehicle deceleration events with peripheral vision: glance response times are independent of visual eccentricity. Accid. Anal. Prev. 150, 105853.
Summala, H., Nieminen, T., Punto, M., 1996. Maintaining lane position with peripheral vision during in-vehicle tasks. Hum. Factors 38 (3), 442–451.
Salvucci, Dario, Goldberg, Joseph, 2000. Identifying fixations and saccades in eye-tracking protocols. Proceedings of the 2000 Symposium on Eye Tracking Research & Applications 71–78.
Savage, S.W., Spano, L.P., Bowers, A.R., 2019. The effects of age and cognitive load on peripheral-detection performance. J. Vis. 19 (1), 15.
Traquair, H.H., 1927. An Introduction to Clinical Perimetry, 1st ed. Henry Kimpton, London.
van Winsum, W., 2018. The effects of cognitive and visual workload on peripheral detection in the detection response task. Hum. Factors 60 (6), 855–869.
Vehtari, A., Gelman, A., Gabry, J., 2017. Practical Bayesian model evaluation using leave-one-out cross-validation and WAIC. Stat. Comput. 27 (5), 1413–1432.
Victor, T.W., Harbluk, J.L., Engström, J.A., 2005. Sensitivity of eye-movement measures to in-vehicle task difficulty. Transp. Res. Part F: Traffic Psychol. Behav. 8 (2), 167–190.
Wood, J.M., 2002. Aging, driving and vision. Clin. Exp. Optometry 85 (4), 214–220.
Wolfe, J.M., 2021. Guided Search 6.0: an updated model of visual search. Psychonomic Bull. Rev. 1–33.
Williams, L.J., 1985. Tunnel vision induced by a foveal load manipulation. Hum. Factors 27 (2), 221–227.
Williams, L.J., 1982. Cognitive load and the functional field of view. Hum. Factors 24 (6), 683–692.
Williams, L.J., 1988. Tunnel vision or general interference? Cognitive load and attentional bias are both important. Am. J. Psychol. 101 (2), 171.
Whelan, R., 2008. Effective analysis of reaction time data. Psychol. Rec. 58 (3), 475–482.
Wolfe, B., Dobres, J., Rosenholtz, R., Reimer, B., 2017. More than the useful field: considering peripheral vision in driving. Appl. Ergon. 65, 316–325.
Wood, J.M., Owsley, C., 2014. Useful field of view test. Gerontology 60 (4), 315–318.
Wolfe, B., Sawyer, B.D., Kosovicheva, A., Reimer, B., Rosenholtz, R., 2019. Detection of brake lights while distracted: separating peripheral vision from cognitive load. Attent. Percept. Psychophys. 81 (8), 2798–2813.
Wolfe, B., Sawyer, B.D., Rosenholtz, R. (2020). Toward a theory of visual information acquisition in driving. *Hum. Factors* 0018720820939693.
Yang, Shiyan, Kuo, Jonny, Lenné, Michael, 2021. Effects of distraction in on-road level 2 automated driving: impacts on glance behavior and takeover performance. Human Factors 63 (8), 1485–1497.
Yang, S., Wilson, K.M., Roady, T., Kuo, J., Lenné, M.G., 2020. Evaluating driver features for cognitive distraction detection and validation in manual and Level 2 automated driving. Hum. Factors.
Yang et al. (2021). Drivers glance like lizards during cell phone distraction in assisted driving. In *Proceedings of Human Factors and Ergonomics Society Annual Meeting, 65* (1), 1410-1414.
Yang, S., Kuo, J., & Lenné, M. G. (2018). Analysis of gaze behavior to measure cognitive distraction in real-world driving. In *Proceedings of the Human Factors and Ergonomics Society Annual Meeting, 62*(1), 1944-1948.